

Theoretical investigation of F₄₃₀-catalyzed dehalogenation of chloro-alkanes. A comprehensive DFT benchmark

Supplementary Information

Dominik Dusza,[†] Mateusz Pokora,[†] Li Ji,[‡] Piotr Paneth^{†,¶*}

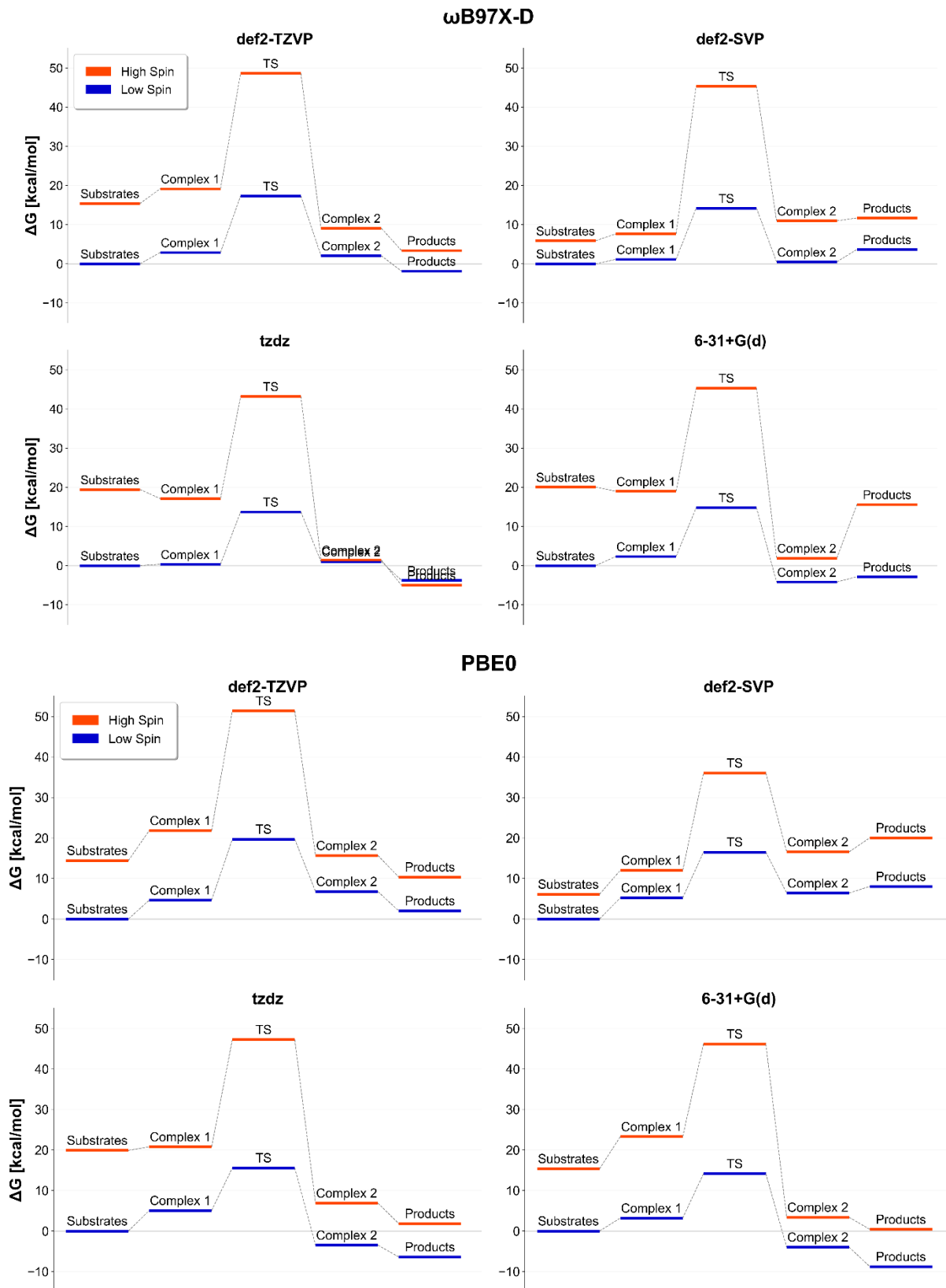
[†]International Center of Research on Innovative Biobased Materials (ICRI-BioM) – International Research Agenda, Lodz University of Technology, Stefanowskiego 2/22, 90-924 Lodz, Poland

[‡]School of Environment Science and Spatial Informatics, China University of Mining and Technology, Xuzhou 221116, China

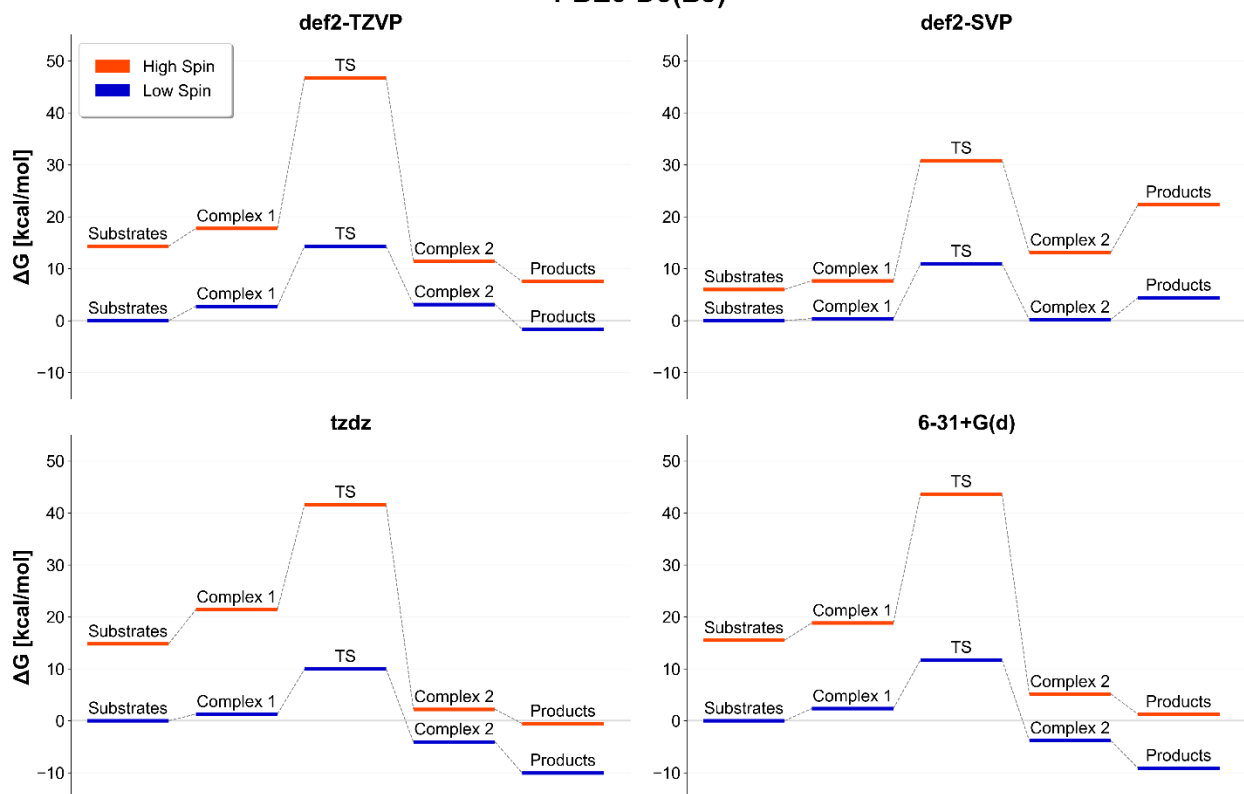
[¶]Institute of Applied Radiation Chemistry, Lodz University of Technology, Zeromskiego 116, 90-537 Lodz, Poland

E-mail: piotr.paneth@p.lodz.pl

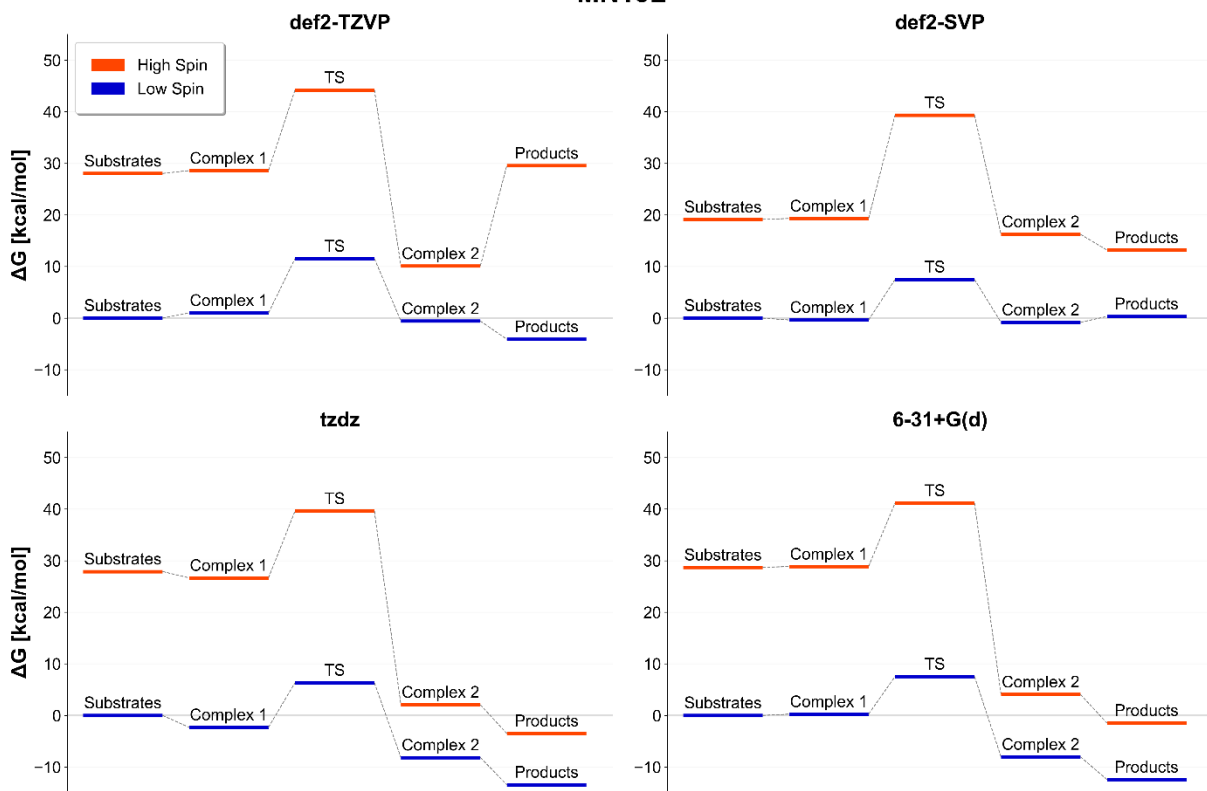
S1. Reaction pathways



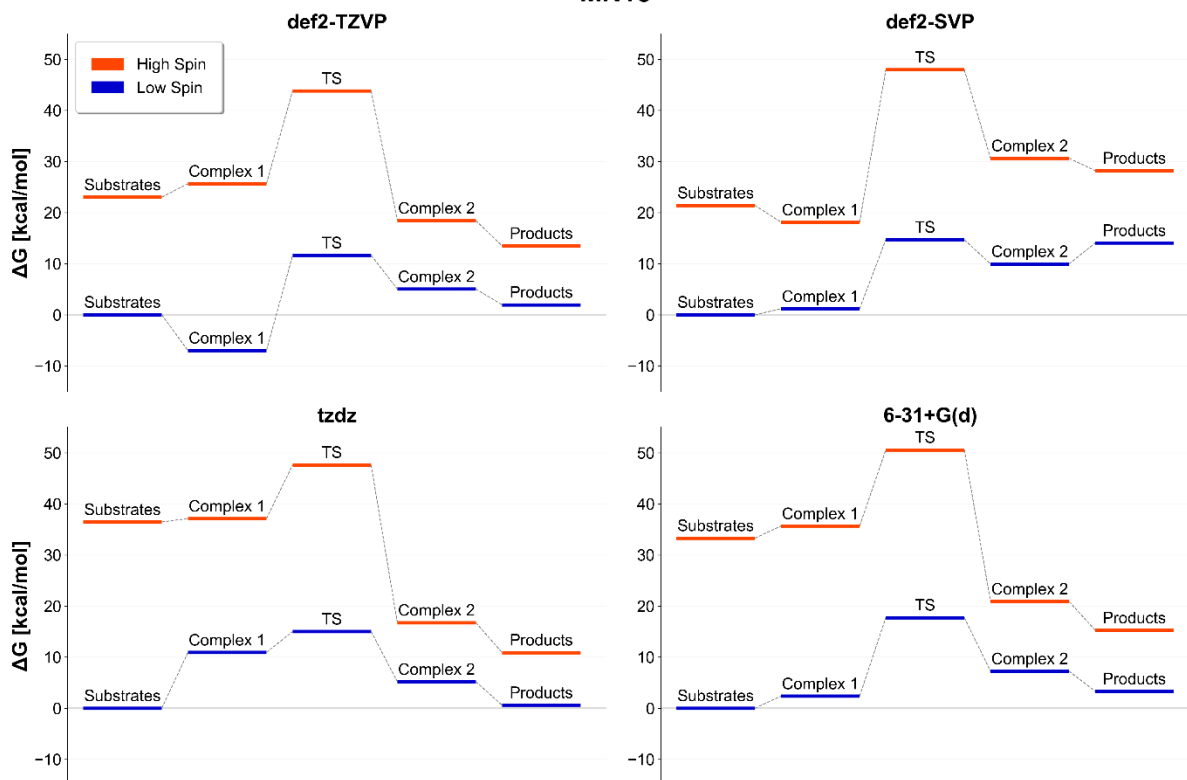
PBE0-D3(BJ)



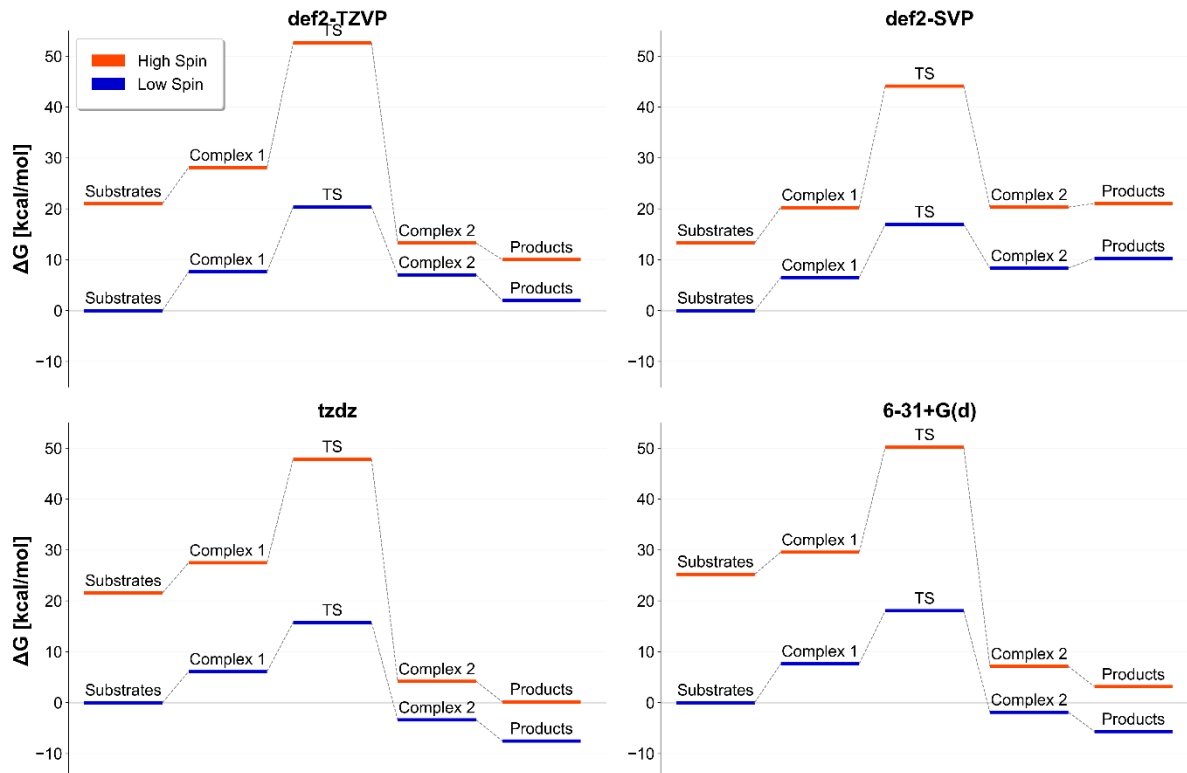
MN15L



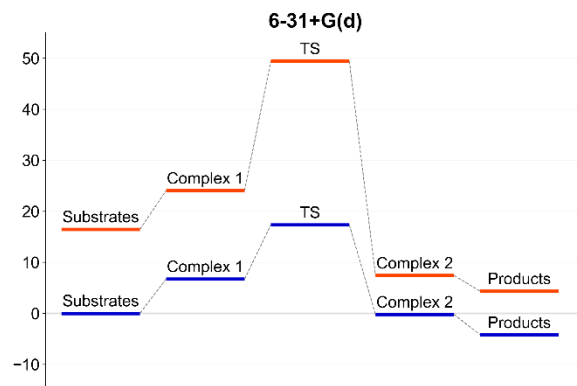
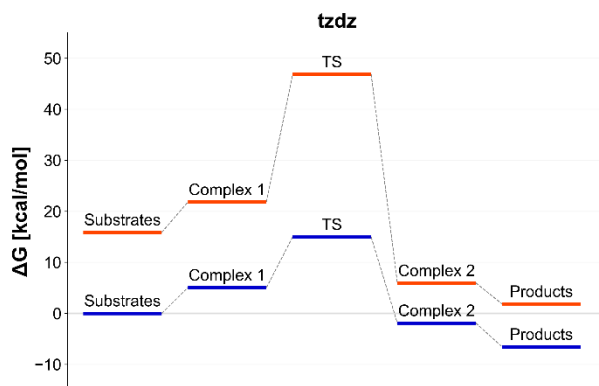
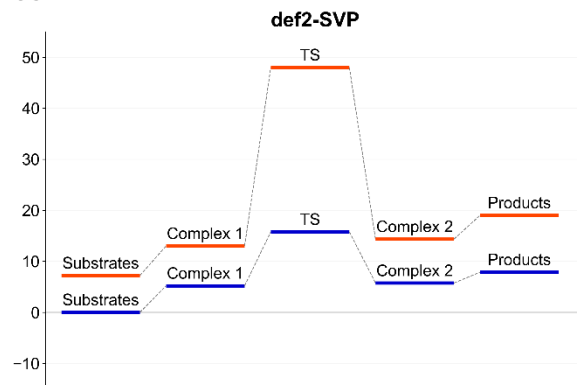
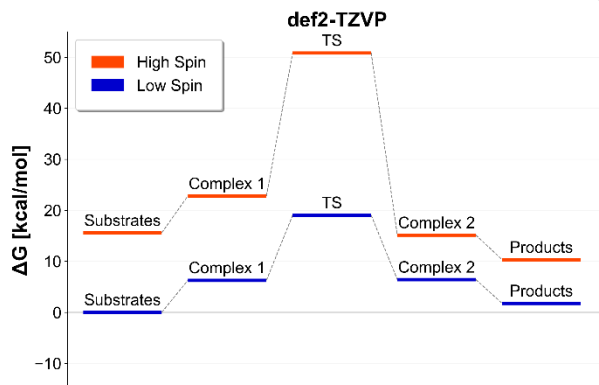
MN15



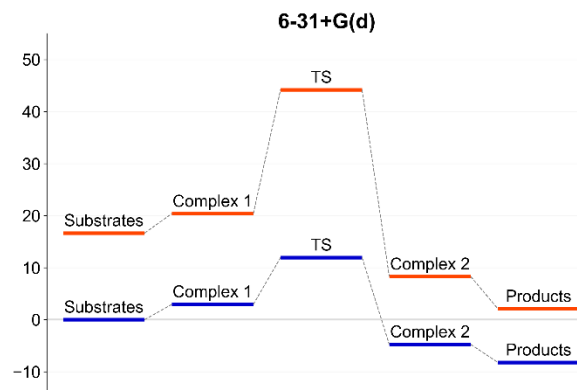
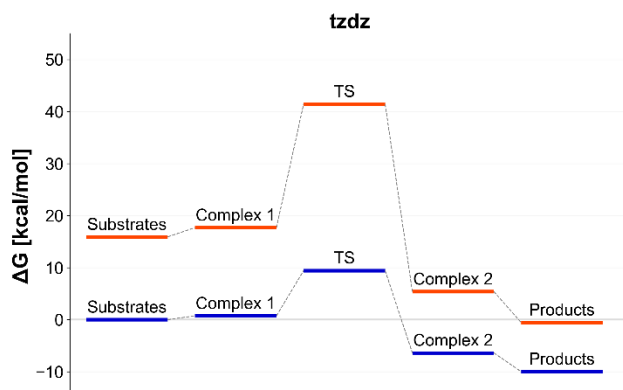
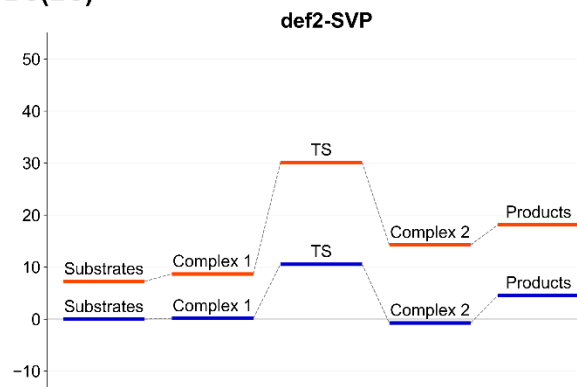
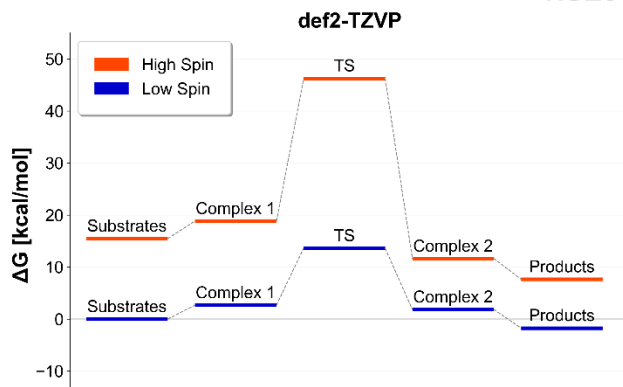
B3LYP



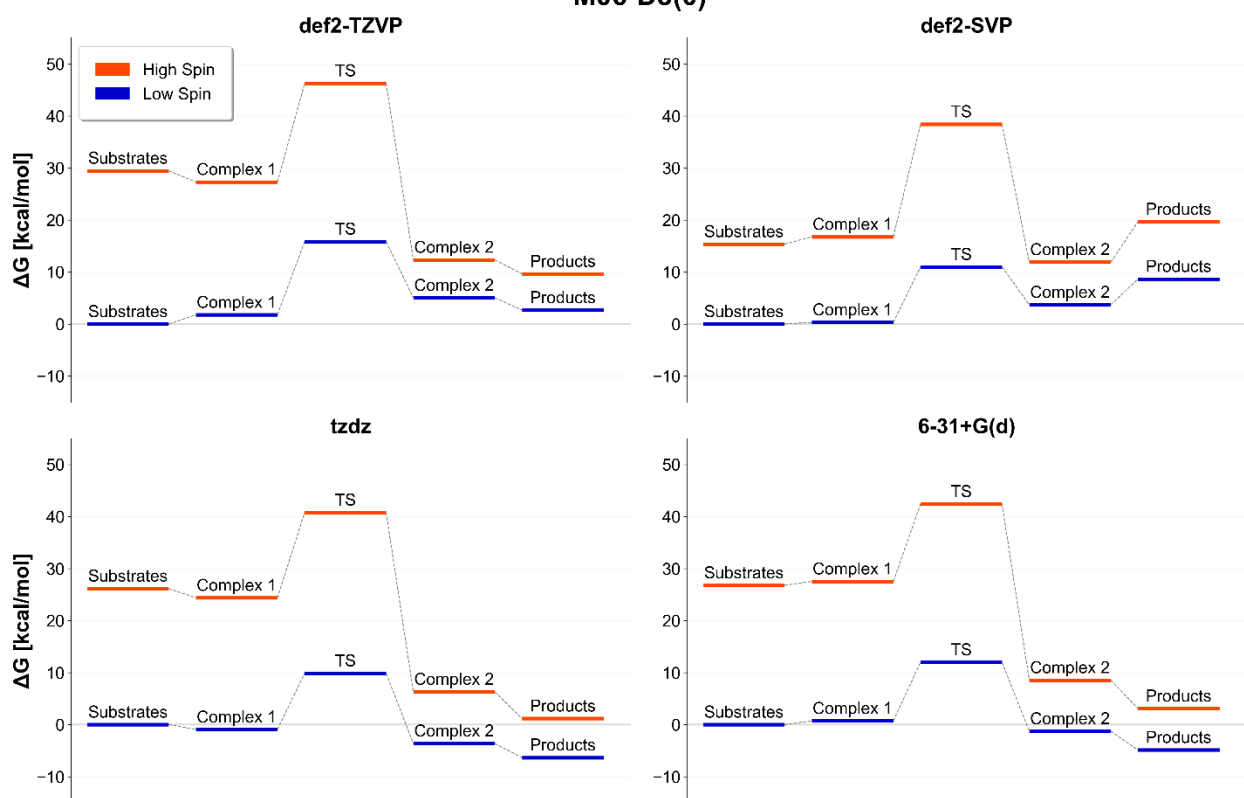
HSE06



HSE06-D3(BJ)



M06-D3(0)



S2. Gibbs free energy of activation

In addition to the functionals mentioned in the main text, ω B97X-V¹ functional combined with def2-TZVP basis set was used in ORCA 5.0.4 software², however, the full reaction path did not converge, hence we report only the Gibbs free energy of activation.

Table S1. ΔG^\ddagger values for considered levels of theory for LS state. tzdz stands for dual basis of 6-311+G(d,p)/6-31+G(d,p).

		ΔG^\ddagger [kcal/mol]			
Experimental		11.87 \pm 1.87			
Basis	Functional	def2-TZVP	def2-SVP	6-31+G(d)	tzdz
	MN15-L	11.52	7.85*	7.56	8.62*
	B3LYP-D3(BJ)	10.68	8.82*	9.20	6.92
	HSE06-D3(BJ)	13.61	10.56	11.93	9.43
	PBE0-D3(BJ)	14.33	10.92	11.71	9.97
	M06-D3(0)	15.82	10.98	11.97	10.78*
	ω B97X-D	17.30	10.98	14.77	13.68
	MN15	18.63*	14.68	17.74	15.01
	HSE06	19.03	15.58	17.32	14.96
	PBE0	19.68	16.51	14.14	15.57
	B3LYP	20.34	16.93	18.04	15.74
	ω B97X-V ^a	22.44	–	–	–
	ω B97M-V ^{a,b}	20.46	–	–	–
	B97M-V ^{a,b}	10.69	–	–	–

*With respect to complex 1. ^aFull reaction path was not obtained. ^bdef2-SVP frequencies with def2-TZVP energies

Table S2. Impact of low-valued frequencies treatment on the Gibbs free energy of activation. $\Delta S(\text{C1-S})$ is the entropy change upon complex formation (with and without Grimme RRHO correction), and $\Delta\Delta S$ is the difference between these two values. ΔG^\ddagger are given in kcal/mol, whereas ΔS in kcal/(mol K)

Functional	ΔG^\ddagger	ΔG^\ddagger	ΔG^\ddagger	ΔG^\ddagger	$\Delta S(\text{S-C1})$	$\Delta S(\text{S-C1})$	$\Delta\Delta S$
		Truhlar	Grimme	Minenkov		Grimme	
B3LYP	19.69	20.81	20.83	19.89	6.33	9.17	2.84
B3LYP-D3	10.68	11.95	11.89	10.95	7.95	9.90	1.96
HSE06	19.04	20.35	20.30	19.32	6.88	9.43	2.54
HSE06-D3	13.61	14.89	14.82	13.92	7.74	9.81	2.07
MN15	18.63	17.75	17.85	18.30	8.51	9.98	1.47
MN15L	11.52	12.84	12.58	11.89	9.25	10.55	1.30
PBE0	19.68	21.01	20.96	19.98	4.99	8.49	3.50
PBE0-D3	14.33	15.44	15.41	14.56	7.72	9.81	2.09
M06-D3	15.83	16.43	16.52	15.85	9.24	10.69	1.44
WB97X-D	17.31	18.69	18.54	17.66	8.42	10.18	1.76

Table S3. The root mean square errors (RMSE) for each functional across all basis sets and for each basis set across all functionals.

Functional/basis set	RMSE
PBE0-D3(BJ)	13.71%
HSE06-D3(BJ)	13.78%
M06-D3(0)	17.67%
ω B97X-D	27.29%
B3LYP-D3(BJ)	27.41%
MN15-L	28.39%
MN15	41.68%
PBE0	42.41%
HSE06	43.02%
B3LYP	51.66%
tzdz	26.26%
def2-SVP	26.43%
6-31+G(d)	31.69%
def2-TZVP	45.01%

The lowest RMSE values are obtained for the PBE0-D3(BJ), HSE06-D3(BJ), and M06-D3(0) functionals. Surprisingly, def2-TZVP basis sets yielded the highest value of RMSE of 45.01%. As

illustrated in **Figure 3**, the def2-TZVP basis set exhibits a considerable number of high-valued outliers, predominantly arising from functionals lacking dispersion correction. However, when only functionals that handle dispersion interactions are considered (B3LYP/HSE06/PBE0/M06-D3, MN15L, and ω B97X-D), the RMSE values decrease to 25.67%, 18.73%, 20.10%, and 24.10% for def2-TZVP, def2-SVP, 6-31+G(d) and tzd, respectively, and while the discrepancy between the basis sets is significantly reduced, def2-TZVP still exhibits the highest value. Additionally, we performed a timing benchmark (**Table S3**) to shed additional insight into the technical aspect of the computations.

Table S4. Timings of TS harmonic vibrational analysis for the best 11 levels of theory as run on 2 x 24 cores Intel Xeon Platinum 8268 machine along with relative errors of ΔG^\ddagger .

Level of theory	Time [h]	RE [%]
PBE0-D3(BJ)/def2-SVP	1.81	-8.00%
M06-D3(0)/def2-SVP	2.31	-7.50%
HSE06-D3(BJ)/def2-SVP	3.08	-11.04%
HSE06-D3(BJ)/6-31+G(d)	4.89	0.51%
MN15-L/def2-TZVP	6.17	-2.95%
PBE0-D3(BJ)/6-31+G(d)	8.43	-1.35%
M06-D3(0)/6-31+G(d)	9.42	0.84%
ω B97X-D/tzd	10.73	15.25%
HSE06-D3(BJ)/def2-TZVP	12.34	14.66%
M06-D3(0)/tzd	13.97	-9.18%
B3LYP-D3/def2-TZVP	16.07	-10.03%

Without any surprise, the def2-SVP basis set requires the least amount of time, being followed by 6-31+G(d); similar timings were obtained for tzd and def2-TZVP. Surprisingly, the MN15-L/def2-TZVP is placed among the 6-31+G(d) basis sets, outperforming the remaining two functionals (HSE06-D3(BJ) and B3LY-D3(BJ)) by 6.17 h and 9.90 h. Based on the presented values, the average time required to finish the frequency task for each basis sets can be estimated as: 2.40 hours for def2-SVP, 7.58 hours for 6-31+G(d), 11.53 hours for def2-TZVP, and 13.15 hours for tzd.

S3. Significance of dispersion correction

In the publication of Szatkowski and Hall,³ the usage of B3LYP functional without the empirical dispersion yielded better results. The authors utilized smaller model of F₄₃₀, namely isobacteriochlorin (iBCh) model, which lacks the side ethyl groups present in the OEt*i*BCh model. We decided, therefore, to perform the IRI analysis of the iBCh structure which is presented in **Figure S1**.

In the case of the substrate, as expected, we do not observe any green surfaces which would indicate dispersive interactions. In the transition state, however, the appearance of green surfaces indicates interactions between the carbon atom of the methyl group and nitrogen atoms. Additionally, interactions between the carbon atom of the methyl group and the carbon atom connecting the pyrrolidine rings are observed, which is a more surprising result. While the dispersion plays a less significant role than in the case of OEt*i*BCh, it appears to exert a notable influence on the stabilization of the transition state.

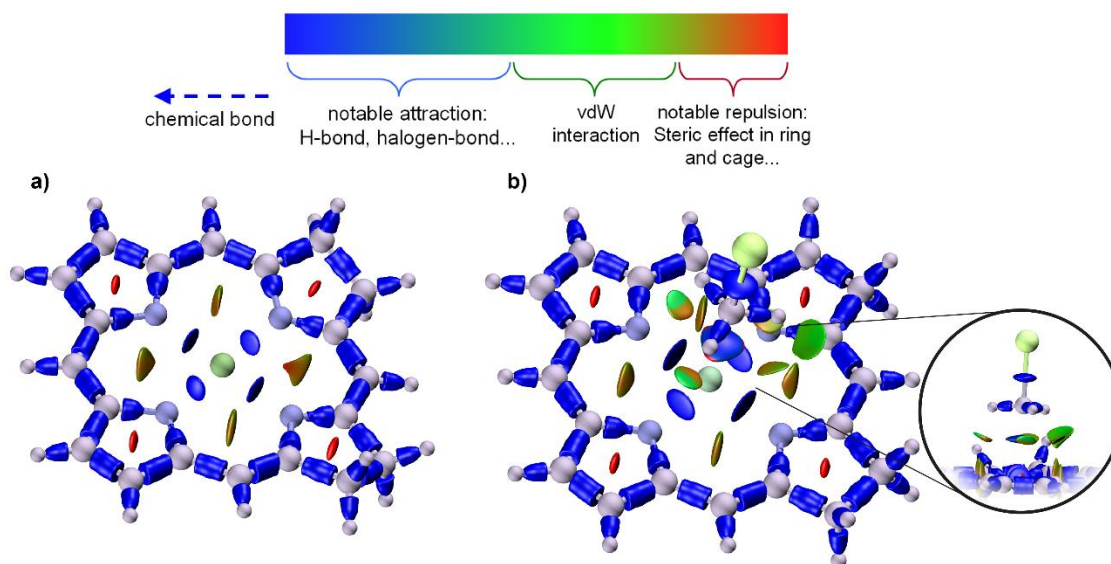


Figure S1. Visualization of the interaction region indicator (IRI) for the iBCh model. Both structures of a) substrate and b) TS are taken from the ω B97X-D/tzdz level of theory.

S4. Impact of the planarity of the porphyrin ring

In our preliminary calculations, we sought to reproduce the findings of Szatkowski and Hall,³ focusing on the isobacteriochlorin (iBCh) model, which lacks the side ethyl groups present in the OEtiBCh model utilized in our study. A notable discrepancy was observed in the case of ω B97X-D/tzdz for the HS state. Szatkowski and Hall reported a ΔG^\ddagger value of 11.16 kcal/mol, which is in contradiction to the value obtained from our calculations (32.26 kcal/mol). The authors kindly provided the structures they had utilized, which we then compared with our own. It was observed that the iBCh substrate exhibited a greater degree of bending (in a manner analogous to the trend described in the main text for def2-SVP). The comparison of both structures is presented in **Figure S2**. The Gibbs free energy of our structure was 20.19 kcal/mol lower with only 0.104 Å of MPP difference.

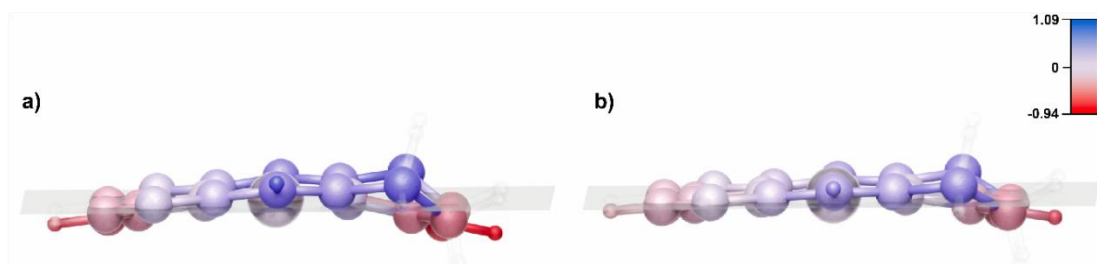


Figure S2. High spin structures of iBCh substrates: a) structure of Szatkowski and Hall with MPP value of 0.308 Å, b) our structure with MPP value of 0.204 Å.

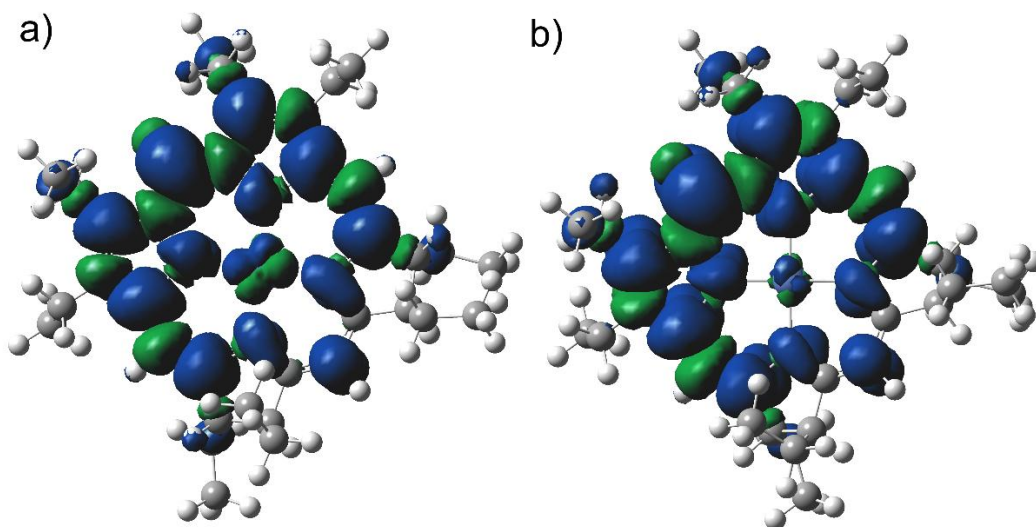


Figure S3. Spin population of MN15/tzdz a) planar, b) distorted structure.

Table S5. Molecular planarity parameter (MPP) values (in Å) for substrates, complex-1 and TS within the LS state.

	Substrates			
	def2-TZVP	def2-SVP	6-31+G(d)	tzdz
Functional				
B3LYP-D3	0.0972	0.1184	0.1023	0.0982
B3LYP	0.1073	0.1269	0.1136	0.1089
HSE06-D3	0.0989	0.1259	0.1078	0.1023
HSE06	0.1039	0.1275	0.1114	0.1069
M06-D3	0.0899	0.1119	0.0950	0.0917
MN15	0.5028	0.5238	0.1052	0.5341
MN15-L	0.0946	0.1193	0.1021	0.0958
PBE0-D3	0.0969	0.1237	0.1058	0.1001
PBE0	0.1051	0.1287	0.1132	0.1079
ω B97X-D	0.0872	0.1123	0.0955	0.0905
	Complex-1			
B3LYP-D3	0.1069	0.1100	0.1133	0.1092
B3LYP	0.1051	0.1133	0.1139	0.1088
HSE06-D3	0.1093	0.1136	0.1214	0.1168
HSE06	0.1050	0.1094	0.1171	0.1118
M06-D3	0.0953	0.0814	0.0796	0.0775
MN15	0.1040	0.518	0.1201	0.5500
MN15-L	0.1189	0.1433	0.1243	0.1203
PBE0-D3	0.1064	0.1143	0.1072	0.1926
PBE0	0.1049	0.1118	0.1185	0.1128
ω B97X-D	0.1008	0.1071	0.1075	0.1029
	TS			
B3LYP-D3	0.1078	0.1313	0.1187	0.1157
B3LYP	0.1076	0.1274	0.1177	0.1129
HSE06-D3	0.1083	0.1300	0.1213	0.1183
HSE06	0.1056	0.1367	0.1201	0.1146
M06-D3	0.0888	0.1061	0.0861	0.0877
MN-5	0.0769	0.1150	0.0870	0.1069
MN15-L	0.0914	0.1268	0.1138	0.0947
PBE0-D3	0.1069	0.1276	0.1201	0.1177
PBE0	0.1070	0.1374	0.1223	0.1161
ω B97X-D	0.0983	0.1253	0.1073	0.1031

S5. Chlorine kinetic isotope effects (Cl-KIEs)

As the isotope effects are particularly sensitive to the geometric parameters, we examined the influence of the C α -Cl bond stretch in the transition state, which was calculated as the difference between the bond length in the TS and that of the complex-1 (see **Table S6**). The values span the range from 0.33 Å to 0.58 Å. The mean elongation of the C α -Cl bond in both the tzdz and 6-31+G(d) basis sets is 0.39 Å. In comparison, the mean values for def2-TZVP and def2-SVP are 0.43 Å and 0.41 Å, respectively. The mean C α -Cl bond length of the transition state appears to be elongated in the def2-TZVP and def2-SVP basis sets with mean values of 2.23 Å and 2.22 Å, respectively. The highest value for each basis set is 2.37 Å and 2.33 Å for MN15 in both cases. In the case of the tzdz and 6-31+G(d), the mean bond lengths are 2.20 Å, with the highest value of 2.32 Å for MN15 in both cases as well.

Since isotopic effects are strongly related to vibrational frequencies, we also compared the predicted frequency of the C-Cl stretching vibration in isolated methyl chloride in the gas phase with the experimental value (see **Table S7**). For the 11 theory of levels that predicted the ΔG^\ddagger values properly, we obtained the following relative errors (RE): -3.19% for PBE0-D3(BJ)/6-31+G(d), -3.67% for MN15-L/def2-TZVP, -1.09% for M06-D3(0)/6-31-G(d), -4.22% for PBE0-D3(BJ)/def2-SVP, -3.04% for B3LYP-D3(BJ)/def2-TZVP, -2.80% for HSE06-D3(BJ)/def2-SVP, -3.55% for ω B97X-D /tzd, -2.98% for HSE0-D3(BJ)/def2-TZVP, -3.20% for HSE0-D3(BJ)/6-31+G(d), -0.51% for M06-D3(0)/tzd, and -3.88% for M06-D3(0)/def2-SVP. Across all the basis sets, the lowest RMSE value was obtained for M06-D3(0) (2.29%), whereas the highest was obtained for ω B97X-D (3.71%). In the cases of basis sets, RMSE values of 2.71%, 3.01%, 3.12%, and 3.54% were acquired for tzd, def2-TZVP, 6-31+G(d), and def2-SVP, respectively.

Table S6. C α -Cl bond stretch in the transition state.

Functional	C α -Cl stretch [\AA]			
	Basis set	def2-TZVP	def2-SVP	6-31+G(d) tzdz
B3LYP-D3(BJ)	0.38	0.38	0.34	0.33
B3LYP	0.41	0.41	0.37	0.36
HSE06-D3(BJ)	0.40	0.38	0.36	0.35
HSE06	0.40	0.38	0.36	0.36
M06-D3(0)	0.49	0.45	0.44	0.43
MN15	0.58	0.55	0.51	0.52
MN15-L	0.47	0.44	0.40	0.42
PBE0-D3(BJ)	0.40	0.38	0.35	0.35
PBE0	0.40	0.37	0.36	0.38
ω B97X-D	0.41	0.38	0.38	0.37

Table S7. Chlorine kinetic isotope effect (Cl-KIE) values and Wiberg bond orders.

Functional	KIE [-]				Wiberg bond order [-]			
	Basis set	def2-TZVP	def2-SVP	6-31+G(d) tzdz	def2-TZVP	def2-SVP	6-31+G(d) tzdz	
B3LYP-D3(BJ)	1.0097	1.0100	1.0091	1.0092	0.58	0.58	0.62	0.63
B3LYP	1.0098	1.0100	1.0096	1.0097	0.55	0.56	0.59	0.60
HSE06-D3(BJ)	1.0113	1.0116	1.0104	1.0102	0.57	0.58	0.60	0.61
HSE06	1.0103	1.0107	1.0100	1.0101	0.57	0.58	0.60	0.60
M06-D3(0)	1.0104	1.0089	1.0097	1.0096	0.50	0.52	0.54	0.54
MN15	1.0101	1.0104	1.0098	1.0099	0.44	0.46	0.48	0.47
MN15-L	1.0103	1.0095	1.0102	1.0104	0.51	0.53	0.56	0.55
PBE0-D3(BJ)	1.0118	1.0118	1.0107	1.0105	0.57	0.59	0.60	0.61
PBE0	1.0117	1.0107	1.0101	1.0102	0.57	0.59	0.60	0.58
ω B97X-D	1.0099	1.0099	1.0096	1.0096	0.56	0.58	0.58	0.59

Table S8. Calculated C–Cl stretching frequencies of isolated MeCl molecule in gas phase. The experimental value of 738.84 cm⁻¹ is taken from [4].

Basis set Functional	def2-TZVP		def2-SVP		6-31+G(d)		tzdz	
	Frequency [cm ⁻¹]	RE [%]						
B3LYP-D3(BJ)	755.11	-3.04%	754.00	0.41%	757.30	-3.34%	754.52	-2.96%
B3LYP	714.62	2.49%	729.80	-3.80%	715.79	2.33%	707.86	3.41%
HSE06-D3(BJ)	754.69	-2.98%	760.70	-4.26%	756.29	-3.20%	749.40	-2.26%
HSE06	758.40	-3.49%	764.03	-2.80%	760.11	-3.72%	753.71	-2.85%
M06-D3(0)	748.42	-2.13%	753.36	-3.88%	740.87	-1.09%	736.55	-0.51%
MN15	754.13	-2.91%	761.26	-5.64%	756.23	-3.19%	748.35	-2.12%
MN15-L	759.75	-3.67%	774.20	-3.79%	761.74	-3.94%	755.25	-3.06%
PBE0-D3(BJ)	754.59	-2.97%	760.60	-4.22%	756.19	-3.19%	749.31	-2.25%
PBE0	758.32	-3.48%	763.73	0.56%	759.83	-3.68%	753.43	-2.81%
ωB97X-D	713.63	2.62%	728.76	2.33%	714.78	2.46%	706.84	3.55%

S7. References

- (1) Mardirossian, N.; Head-Gordon, M. ωB97X-V: A 10-Parameter, Range-Separated Hybrid, Generalized Gradient Approximation Density Functional with Nonlocal Correlation, Designed by a Survival-of-the-Fittest Strategy. *Phys. Chem. Chem. Phys.* **2014**, *16* (21), 9904–9924. <https://doi.org/10.1039/C3CP54374A>.
- (2) Neese, F. Software Update: The ORCA Program System—Version 5.0. *WIREs Computational Molecular Science* **2022**, *12* (5), e1606. <https://doi.org/10.1002/wcms.1606>.
- (3) Szatkowski, L.; Hall, M. B. Dehalogenation of Chloroalkanes by Nickel(I) Porphyrin Derivatives, a Computational Study. *Dalton Trans.* **2016**, *45* (42), 16869–16877. <https://doi.org/10.1039/C6DT02632J>.
- (4) Nikitin, A.; Champion, J. P.; Bürger, H. Global Analysis of 12CH335Cl and 12CH337Cl: Simultaneous Fit of the Lower Five Polyads (0–2600 Cm⁻¹). *Journal of Molecular Spectroscopy* **2005**, *230* (2), 174–184. <https://doi.org/10.1016/j.jms.2004.11.012>.